Supplementary Information for "Seasonality controls on Last Glacial Maximum glacier dynamics in the southern European Alps"

Lukas Rettig[1,2,3] (*), Giovanni Monegato[4], Matteo Spagnolo[5], Brice R. Rea[6], Sarah Kamleitner[7,8], Costanza del Gobbo[9], Susan Ivy-Ochs[7], Adriano Ribolini[10], Franco Gianotti[5], Marcus Christl[7], Christof Vockenhuber[7], Paolo Mozzi[1]

[1]Department of Geosciences, University of Padua, Italy. [2]Laboratory of Hydraulics, Hydrology and Glaciology (VAW), ETH Zürich, Zürich, Switzerland. [3]Swiss Federal Institute for Forest, Snow and Landscape Research (WSL), Bâtiment ALPOLE, Sion, Switzerland. [4]Institute of Geosciences and Earth Resources, National Research Council of Italy, Padua, Italy. [5]Department of Earth Sciences, University of Turin, Italy. [6]Department of Geography and Environment, School of Geosciences, University of Aberdeen, United Kingdom. [7]Laboratory of Ion Beam Physics, ETH Zürich, Zürich, Switzerland. [8]Institute of Earth Surface Dynamics, University of Lausanne, Switzerland. [9]Department of Earth and Atmospheric Sciences, University of Quebec in Montreal, Canada. [10]Department of Earth Sciences, University of Pisa, Italy. (*) Corresponding author (rettig@vaw.baug.ethz.ch).

Summary: This document provides supplementary data, figures and tables to support the main results and conclusions presented in the manuscript. Figures S1 to S4 are illustrations of the four study sites which were investigated for this study: the Inferno Valley (Fig. S1), the Oropa Valley (Fig. S2), Pian Frollero (Fig. S3), and Sella Spa (Fig. S4). Each figure contains several panels with the following information: (A) the location of the site along the southern fringe of the Alps; (B) the regional extent of the Alpine glacier network during the Last Glacial Maximum (LGM) according to previous studies; (C) the reconstruction of the ice surface and Equilibrium Line Altitude (ELA) of the local LGM (l-LGM) glacier; (D) a geomorphological map of the frontal moraine system with the positions of erratic boulders that were sampled for surface exposure dating; and (E-G) selected photographs of the site. Tables S1 and S2 provide further details of the sampled boulders, as well as measured ^{10}Be and ^{36}Cl concentrations and the calculated exposure ages. Concentrations of major and trace elements that were needed to compute different pathways of ^{36}Cl production are listed in Table S3. In Table S4, some important physical characteristics and the calculated ELAs of all 16 reconstructed marginal l-LGM glaciers are reported. This includes the four glaciers presented in Fig. S1 to Fig. S4 and previously published data in Rettig et al. (2023) and Rettig et al. (2024). Table S5 provides additional information on the results of the paleoclimatic analyses that were based on the calculated ELAs and on the regional climate model (RCM) data from Del Gobbo et al. (2023) and Russo et al. (2024).

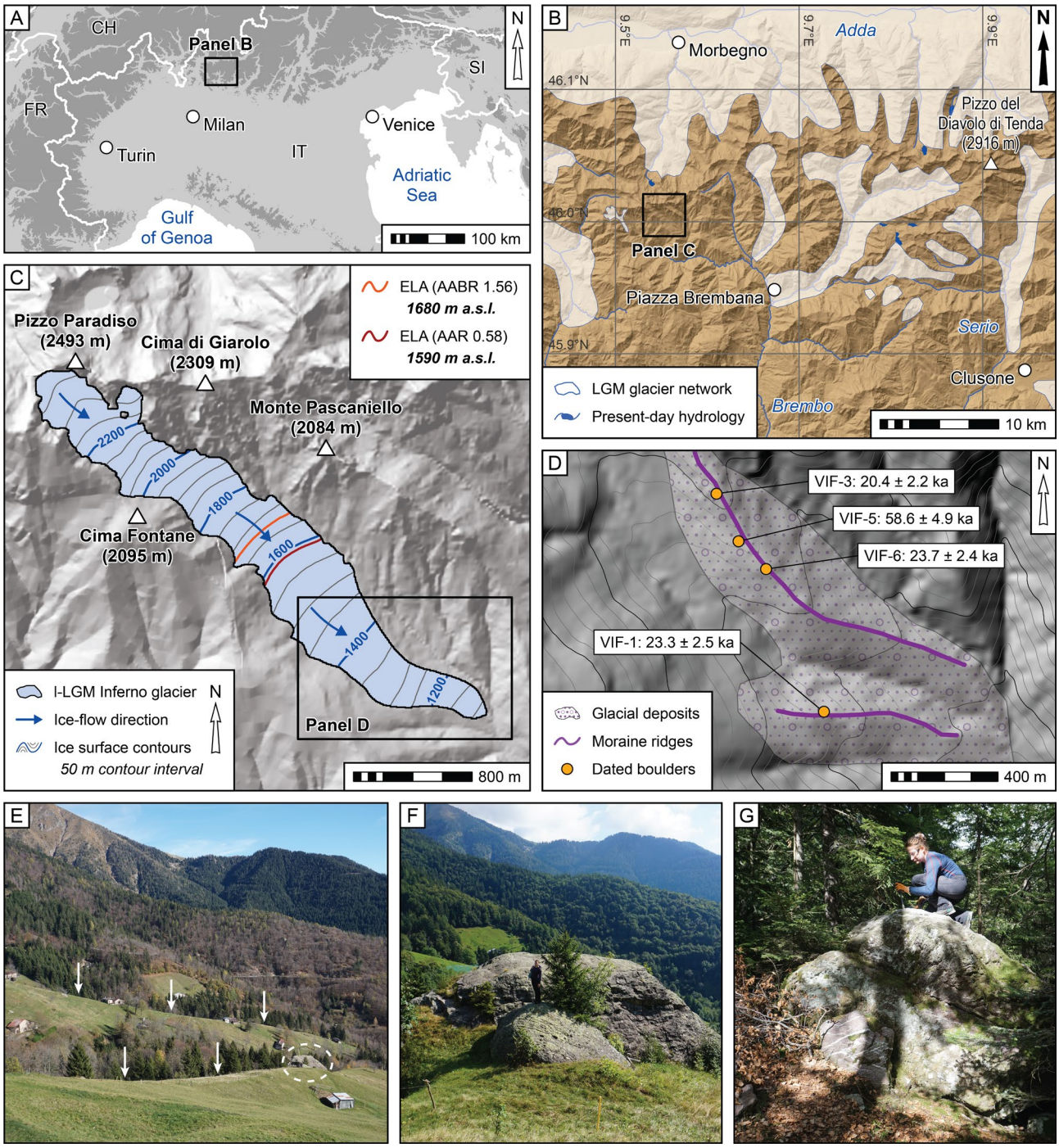

Fig. S1. The study site in the Inferno Valley (province of Bergamo, Lombardy, Italy). **A.** Location of the site along the southern fringe of the Alps. **B**. Regional extent of the LGM glacier network (from Ehlers et al., 2011). **C.** Reconstruction of the ice surface and ELA of the l-LGM Inferno glacier. ELAs were calculated using both an area-altitude balance ratio (AABR) of 1.56 and an accumulation area ratio (AAR) of 0.58 (Oien et al., 2021). **D.** Map of the frontal moraine system in the lower Inferno Valley with the positions of boulders that were sampled for ^{36}Cl surface exposure dating. **E.** View towards the frontal moraine system, the crests of the right (foreground) and left (background) moraine ridge are marked with white arrows. Encircled by a dashed white line is boulder VIF-1. **F.** Boulder VIF-1, the largest exposure-dated boulder in the moraine system. **G.** Sampling of boulder VIF-6 on the crest of the left lateral moraine. Source of the elevation data in all map panels: Copernicus GLO-30 DEM (https://doi.org/10.5270/ESA-c5d3d65) and DTM 5x5 Regione Lombardia (https://www.geoportale.regione.lombardia.it).

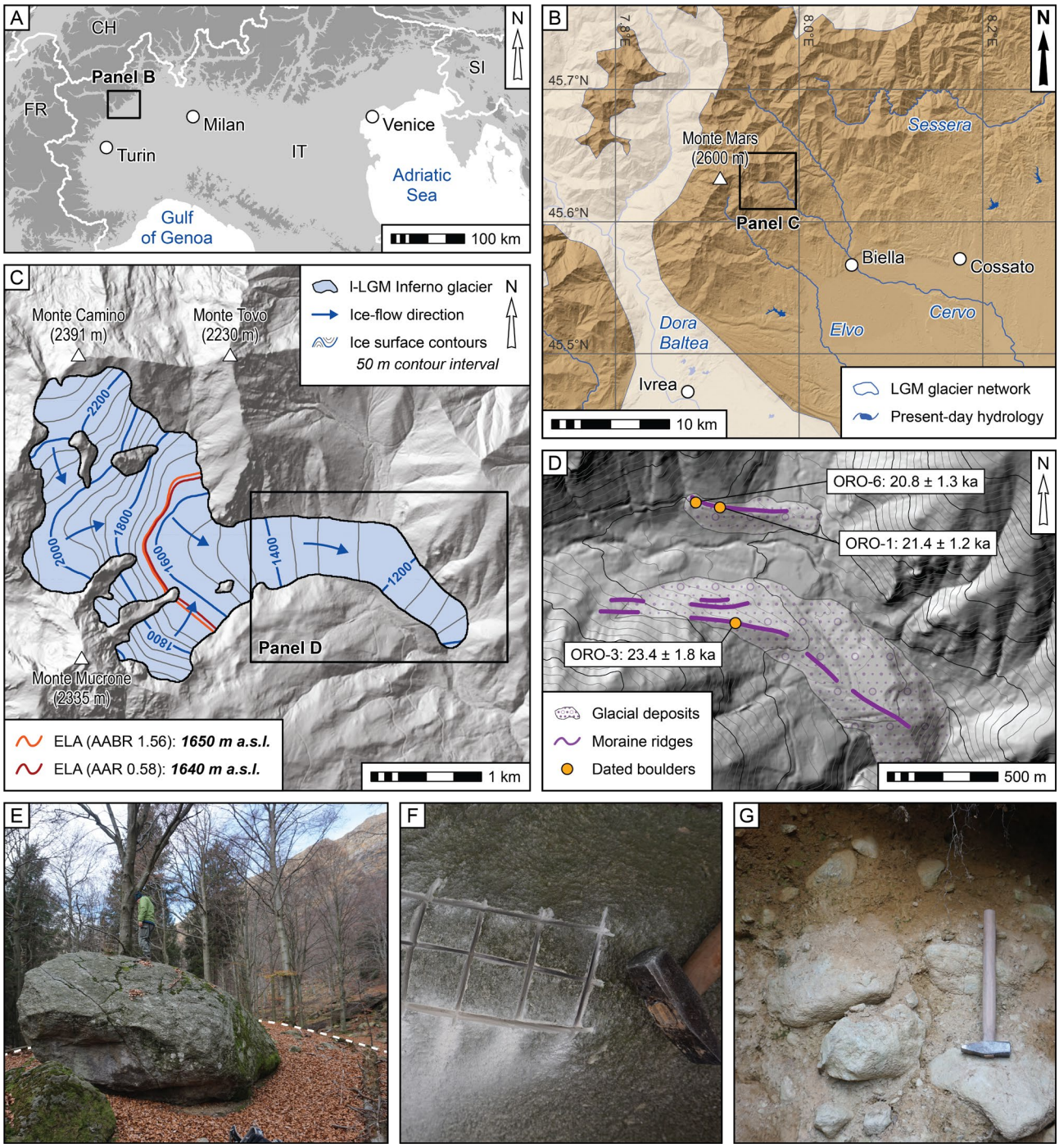

Fig. S2. The study site in the Oropa Valley (province of Biella, Piedmont, Italy). **A.** Location of the site along the southern fringe of the Alps. **B**. Regional extent of the LGM glacier network (from Ehlers et al., 2011). **C.** Reconstruction of the ice surface and ELA of the l-LGM Oropa glacier. ELAs were calculated using both an area-altitude balance ratio (AABR) of 1.56 and an accumulation area ratio (AAR) of 0.58 (Oien et al., 2021). **D.** Map of the frontal moraine system in the lower Oropa Valley with the positions of boulders that were sampled for ^{10}Be surface exposure dating. **E.** The large boulder ORO-1 on the crest of the left lateral moraine. The surface of the moraine ridge is marked with a dashed white line. **F.** Sampling a boulder for exposure dating by sawing a rectangular grid into the rock surface. **G.** Sediment outcrop in the left lateral moraine: clast supported diamict with edge-rounded clasts that indicate a glacial transport history. Source of the elevation data in all map panels: Copernicus GLO-30 DEM (https://doi.org/10.5270/ESA-c5d3d65) and RIPRESA AEREA ICE 2009-2011 - DTM 5 (Regione Piemonte, https://www.geoportale.piemonte.it/).

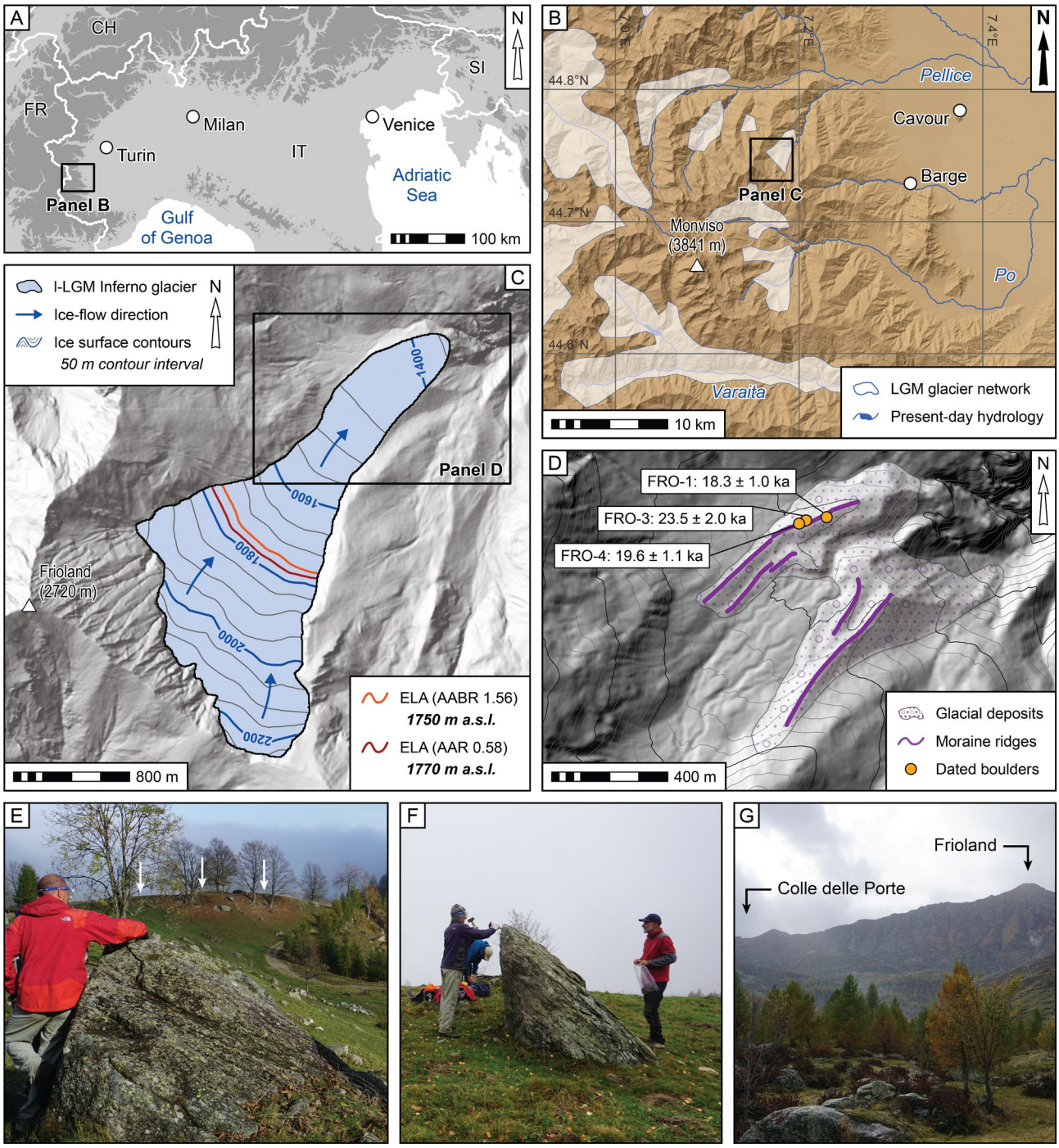

Fig. S3. The study site of Pian Frollero (province of Cuneo, Piedmont, Italy). **A.** Location of the site along the southern fringe of the Alps. **B**. Regional extent of the LGM glacier network (from Ehlers et al., 2011). **C.** Reconstruction of the ice surface and ELA of the l-LGM Frollero glacier. ELAs were calculated using both an area-altitude balance ratio (AABR) of 1.56 and an accumulation area ratio (AAR) of 0.58 (Oien et al., 2021). **D.** Map of the frontal moraine system at Pian Frollero with the positions of boulders that were sampled for ^{10}Be surface exposure dating. **E.** View from inside the moraine system towards the crest of the left lateral moraine ridge. The crest is marked with white arrows. **F.** Sampling the surface of boulder FRO-4 for exposure dating. **G.** View towards Colle delle Porte and Frioland (2720 m) in the former accumulation area of the l-LGM Frollero glacier. Source of the elevation data in all map panels: Copernicus GLO-30 DEM (https://doi.org/10.5270/ESA-c5d3d65) and RIPRESA AEREA ICE 2009-2011 - DTM 5 (Regione Piemonte, https://www.geoportale.piemonte.it/).

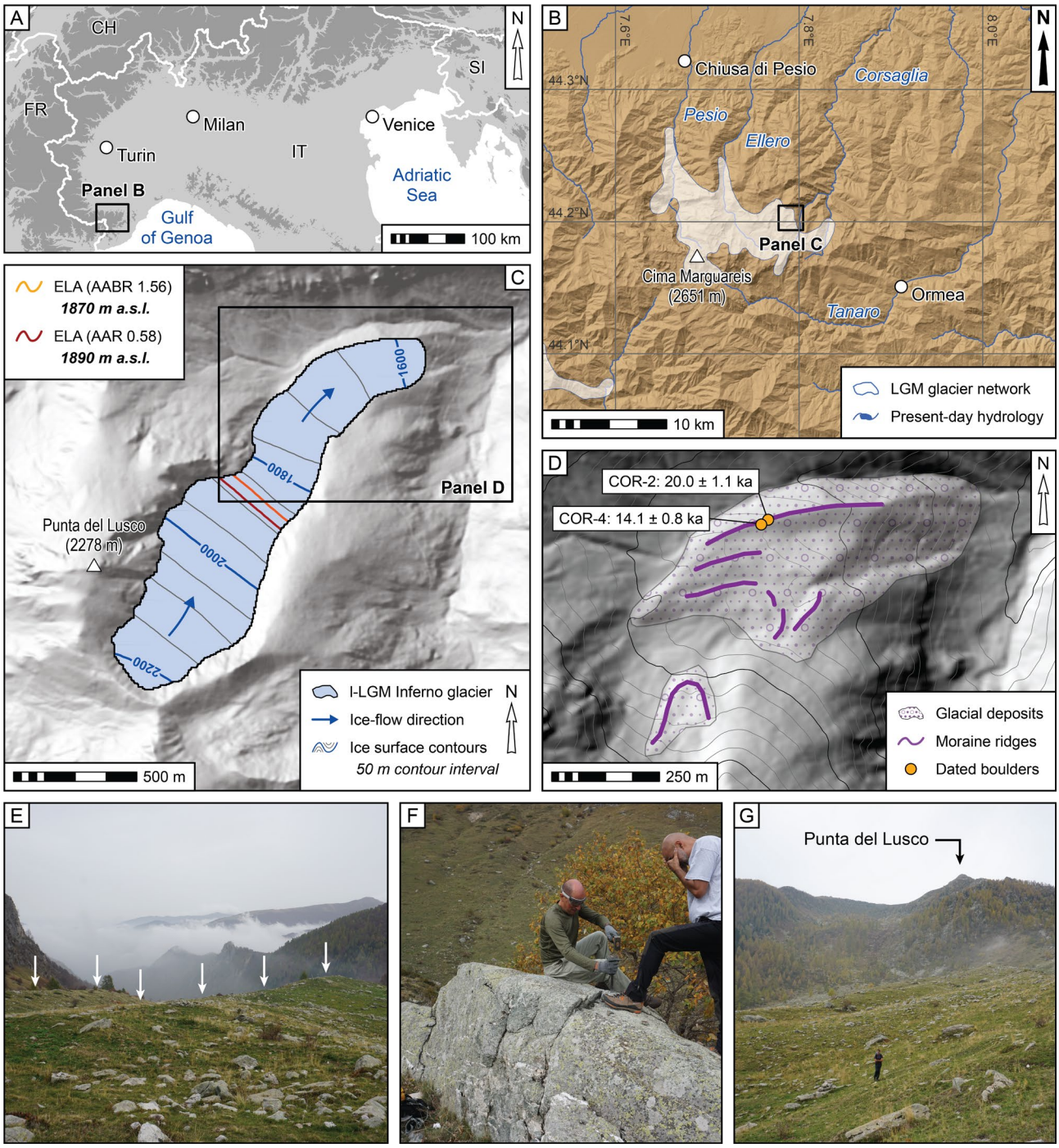

Fig. S4. The study site of Sella Spa (province of Cuneo, Piedmont, Italy). **A.** Location of the site along the southern fringe of the Alps. **B**. Regional extent of the LGM glacier network (from Ehlers et al., 2011). **C.** Reconstruction of the ice surface and ELA of the l-LGM Spa glacier. ELAs were calculated using both an area-altitude balance ratio (AABR) of 1.56 and an accumulation area ratio (AAR) of 0.58 (Oien et al., 2021). **D.** Map of the frontal moraine system at Sella Spa with the positions of boulders that were sampled for ^{10}Be surface exposure dating. **E.** View from inside the moraine system towards the crests of the inner (foreground) and outer (background) left moraine ridge, marked with white arrows. **F.** Sampling the surface of a boulder at Sella Spa for exposure dating. This specific boulder was ultimately not dated. **G.** View towards the small cirque to the east of Punta del Lusco (2278 m), that represents the former accumulation area of the l-LGM Spa glacier. Source of the elevation data in all map panels: Copernicus GLO-30 DEM (https://doi.org/10.5270/ESA-c5d3d65) and RIPRESA AEREA ICE 2009-2011 - DTM 5 (Regione Piemonte, https://www.geoportale.piemonte.it/).

Table S1. Sample details of ^{10}Be exposure dated boulders from the l-LGM moraine systems in the lower Oropa Valley (ORO), at Pian Frollero (FRO), and at Sella Spa (COR). The calculated exposure ages are reported both with internal and external 1σ errors (in brackets).

	Boulder size (L x W x H) [m]	Boulder coordinates [°N]	[°E]	Elevation [m a.s.l.]	Sample thickness [cm]	Topographic shielding factor	^{10}Be concentration [*10^5 at g^{-1}]	Exposure age 1 mm/ka erosion [ka]	Exposure age 0 mm/ka erosion [ka]
ORO-1	5.0 x 5.0 x 2.5	45.6316	7.9744	1290	1.9	0.9772	2.372 ± 0.072	21.4 ± 0.7 (1.2)	21.0 ± 0.6 (1.2)
ORO-3	2.5 x 2.0 x 1.7	45.6269	7.9753	1260	2.0	0.9714	2.516 ± 0.138	23.4 ± 1.3 (1.8)	23.0 ± 1.3 (1.7)
ORO-6	3.0 x 2.5 x 1.5	45.6318	7.9730	1300	2.2	0.9708	2.309 ± 0.083	20.8 ± 0.8 (1.3)	20.5 ± 0.7 (1.2)
FRO-1	2.5 x 2.0 x 1.6	44.7592	7.1812	1410	1.9	0.9851	2.229 ± 0.064	18.3 ± 0.5 (1.0)	18.1 ± 0.5 (1.0)
FRO-3	2.0 x 1.3 x 0.9	44.7591	7.1803	1420	2.9	0.9837	2.822 ± 0.190	23.5 ± 1.6 (2.0)	23.0 ± 1.6 (1.9)
FRO-4	3.5 x 3.0 x 1.7	44.7590	7.1800	1420	2.7	0.9832	2.370 ± 0.058	19.6 ± 0.5 (1.1)	19.3 ± 0.5 (1.0)
COR-2	3.0 x 2.5 x 0.6	44.2096	7.7951	1640	3.0	0.9590	2.760 ± 0.071	20.0 ± 0.5 (1.1)	19.6 ± 0.5 (1.1)
COR-4	1.5 x 1.0 x 0.3	44.2095	7.7949	1650	2.5	0.9658	1.981 ± 0.043	14.1 ± 0.3 (0.8)	13.9 ± 0.3 (0.7)

Table S2. Sample details of ^{36}Cl exposure dated boulders from the l-LGM moraine system in the lower Inferno Valley (VIF). The calculated exposure ages are reported both with internal and external 1σ errors (in brackets).

	Boulder size (L x W x H) [m]	Boulder coordinates [°N]	[°E]	Elevation [m a.s.l.]	Sample thickness [cm]	Topographic shielding factor	^{36}Cl concentration [*10^5 at g^{-1}]	Exposure age 1 mm/ka erosion [ka]	Exposure age 0 mm/ka erosion [ka]
VIF-1	21 x 9.0 x 7.0	45.9942	9.5659	1240	2.5	0.9814	6.725 ± 0.407	23.3 ± 1.5 (2.5)	24.4 ± 1.5 (2.5)
VIF-3	8.0 x 8.0 x 4.0	45.9997	9.5620	1410	2.5	0.9754	5.310 ± 0.510	20.4 ± 2.0 (2.2)	20.6 ± 2.0 (2.2)
VIF-5	4.0 x 3.0 x 4.5	45.9985	9.5628	1370	1.5	0.9778	16.660 ± 0.916	58.6 ± 3.4 (4.9)	61.8 ± 3.4 (4.8)
VIF-6	3.0 x 3.5 x 2.0	45.9978	9.5638	1350	1.5	0.9801	5.573 ± 0.490	23.7 ± 2.1 (2.4)	24.0 ± 2.1 (2.4)

Table S3. Concentrations of major and trace elements of samples from the lower Inferno Valley (VIF), necessary to compute the different pathways of ^{36}Cl production. The element concentrations were determined from a leached sample aliquot by Activation Laboratories Ltd (Ontario, Canada).

	Al_2O_3 [wt%]	CaO [wt%]	Fe_2O_3 [wt%]	K_2O [wt%]	MgO [wt%]	MnO [wt%]	Na_2O [wt%]	P_2O_5 [wt%]	SiO_2 [wt%]	TiO_2 [wt%]	LOI [wt%]	Gd [ppm]	Sm [ppm]	Th [ppm]	U [ppm]	Cl [ppm]
VIF-1	12.43	0.11	2.90	3.36	0.59	0.018	3.80	0.02	73.80	0.436	1.44	2.6	3.5	8.2	2.6	129.5
VIF-3	9.31	0.05	2.69	4.64	0.49	0.011	0.69	0.01	79.89	0.214	1.12	4.2	5.9	8.9	1.9	46.4
VIF-5	8.80	0.05	3.16	4.52	0.36	0.010	0.99	0.01	79.96	0.184	1.02	3.8	5.4	8.5	2.0	75.0
VIF-6	8.11	0.04	3.44	4.28	0.38	0.010	0.72	0.02	80.81	0.182	0.87	4.0	4.9	9.0	2.2	49.5

Table S4. Physical characteristics and ELAs of the 16 reconstructed marginal l-LGM glaciers. Glaciers marked with (1) are from Rettig et al. (2023) and glacier marked with (2) from Rettig et al. (2024). Underlined glaciers are here presented for the first time in the supplementary information (Figures S1 to S4). Glaciers 1-8 are in the south-eastern Alps, glaciers 9-11 in the south-central Alps and glaciers 12-16 in the south-western Alps.

ID	Glacier name (Reference)	Glacier type	Lat [°N]	Long [°E]	Elevation range [m a.s.l.]	Surface area [km^2]	Ice volume [km^3]	JJA solar radiation [kWh/m^2]	ELA AABR 1.56 [m a.s.l.]	ELA AAR 0.58 [m a.s.l.]
1	Vodizza (1)	Valley glacier	46.31	13.25	640-1580	1.8	0.06	479 ± 56	1140 ± 65	1120 ± 65
2	Bombasine (1)	Valley glacier	46.31	13.22	500-1620	4.2	0.14	461 ± 55	1160 ± 65	1210 ± 65
3	Pozzus (1)	Valley glacier	46.31	13.19	600-1740	1.7	0.05	439 ± 68	1090 ± 65	1070 ± 65
4	Monte Raut (1)	Valley glacier(s)	46.24	12.67	440-2030	7.0	0.23	486 ± 62	1260 ± 65	1370 ± 65
5	Castelat (1)	Plateau glacier	46.16	12.57	580-1660	12.4	0.75	524 ± 51	1330 ± 65	1440 ± 65
6	Monte Cavallo (1)	Valley glacier(s)	46.12	12.51	500-2060	24.4	1.42	525 ± 61	1330 ± 65	1360 ± 65
7	Meatte (1)	Cirque glacier	45.89	11.83	1320-1620	0.3	0.01	491 ± 49	1460 ± 65	1470 ± 65
8	Monte Grappa (1)	Ice cap	45.88	11.80	900-1810	12.3	0.47	529 ± 54	1450 ± 65	1460 ± 65
9	Sette Comuni (1)	Plateau glacier	45.96	11.53	900-2300	98.3	9.85	568 ± 46	1690 ± 65	1690 ± 65
10	Inferno	Valley glacier	46.00	9.55	1070-2370	1.5	0.06	542 ± 54	1680 ± 65	1590 ± 65
11	Oropa	Valley glacier	45.63	7.96	990-2340	4.4	0.17	530 ± 61	1650 ± 65	1640 ± 65
12	Frollero	Cirque glacier	44.75	7.17	1340-2270	2.3	0.08	498 ± 56	1750 ± 65	1770 ± 65
13	Costa Ganola (2)	Cirque glacier	44.21	7.41	1190-2100	1.0	0.03	451 ± 61	1620 ± 65	1590 ± 65
14	Caramagne (2)	Valley glacier	44.13	7.52	1150-2620	5.0	0.26	564 ± 69	1980 ± 65	2040 ± 65
15	Limonetto (2)	Valley glacier	44.16	7.54	1090-2610	9.3	0.64	511 ± 65	1790 ± 65	1790 ± 65
16	Spa	Cirque glacier	44.20	7.79	1570-2230	0.6	0.02	493 ± 63	1870 ± 65	1890 ± 65

Table S5. Results of the palaeoclimatic analyses that were carried out for all 16 sites of marginal l-LGM glaciation. The calculated palaeoprecipitation sums (P_{ELA}) are based on reconstructed ELAs (see Table S4) and (1) T_{JJA} during the pre-industrial (PI), retrieved from the HISTALP dataset (Auer et al., 2007), (2) ΔT_{JJA} between PI and the LGM, based on the RCM by Del Gobbo et al. (2022), and the empirical P/T relationships by (3) Ohmura and Boettcher (2018) and (4) Golledge et al. (2010) with a seasonality factor of 0.8. In comparison: RCM-based precipitation estimates from Del Gobbo et al. (2022) and (5) Russo et al. (2024).

ID	Glacier name	ELA AABR 1.56 [m a.s.l.]	T_{JJA} (PI) sea level (1) [°C]	ΔT_{JJA} PI-LGM (2) [°C]	T_{JJA} (LGM) at ELA [°C]	P_{ELA} - *neutral seasonality* (3) [mm/yr]	P_{ELA} - *winter seasonality* (4) [mm/yr]	P_{RCM} (2) [mm/yr]	P_{RCM} (5) [mm/yr]
1	Vodizza	1140 ± 65	21.7 ± 0.6	6.6	7.7 ± 0.8	3070 ± 670	2360 ± 550	2060	1870
2	Bombasine	1160 ± 65	21.6 ± 0.6	6.6	7.4 ± 0.7	3000 ± 670	2270 ± 550	2060	1880
3	Pozzus	1090 ± 65	21.4 ± 0.6	6.4	7.9 ± 0.7	3160 ± 670	2460 ± 550	1990	1810
4	Monte Raut	1260 ± 65	21.7 ± 0.6	6.7	6.7 ± 0.7	2780 ± 670	2030 ± 550	1990	1810
5	Castelat	1330 ± 65	22.1 ± 0.6	6.4	7.1 ± 0.8	2880 ± 670	2140 ± 550	1940	1960
6	Monte Cavallo	1330 ± 65	21.8 ± 0.6	5.8	7.4 ± 0.8	2980 ± 670	2250 ± 550	1810	2270
7	Meatte	1460 ± 65	22.2 ± 0.7	5.9	6.9 ± 0.8	2820 ± 680	2070 ± 550	1500	1990
8	Monte Grappa	1450 ± 65	22.3 ± 0.6	5.9	7.0 ± 0.8	2850 ± 670	2100 ± 550	1500	1970
9	Sette Comuni	1690 ± 65	22.0 ± 0.7	7.6	3.4 ± 0.8	1820 ± 680	990 ± 550	1180	1640
10	Inferno	1680 ± 65	22.3 ± 0.7	7.5	3.8 ± 0.9	1930 ± 680	1100 ± 550	1290	1770
11	Oropa	1650 ± 65	22.5 ± 0.7	6.5	5.3 ± 0.8	2340 ± 680	1530 ± 550	1880	1770
12	Frollero	1750 ± 65	23.1 ± 0.7	6.5	5.2 ± 0.8	2320 ± 680	1510 ± 550	1000	1420
13	Costa Ganola	1620 ± 65	23.2 ± 0.8	6.5	6.3 ± 0.9	2640 ± 680	1860 ± 550	1420	1490
14	Caramagne	1980 ± 65	23.4 ± 0.8	6.7	3.9 ± 0.9	1950 ± 680	1120 ± 550	1300	1830
15	Limonetto	1790 ± 65	23.5 ± 0.7	6.7	5.2 ± 0.9	2310 ± 680	1500 ± 550	1300	2050
16	Spa	1870 ± 65	23.3 ± 0.7	6.4	4.8 ± 0.9	2200 ± 680	1380 ± 550	1420	1990